FRONTIERS OF PHYSICS

RESEARCH ARTICLE
Volume 19 / Issue 2 / 22201 / 2024

Universal dynamic scaling and Contact dynamics in quenched quantum gases

Jia-Nan Cui[1], Zhengqiang Zhou[1], Mingyuan Sun[1,2,†]

1 School of Science, Beijing University of Posts and Telecommunications, Beijing 100876, China
2 State Key Lab of Information Photonics and Optical Communications, Beijing University of Posts and Telecommunications, Beijing 100876, China
Corresponding author. E-mail: †mingyuansun@bupt.edu.cn
Received July 11, 2023; accepted August 24, 2023

ABSTRACT

Recently universal dynamic scaling is observed in several systems, which exhibit a spatiotemporal self-similar scaling behavior, analogous to the spatial scaling near phase transition. The latter one arises from the emergent continuous scaling symmetry. Motivated by this, we investigate the possible relation between the scaling dynamics and the continuous scaling symmetry in this paper. We derive a theorem that the scaling invariance of the quenched Hamiltonian and the initial density matrix can lead to the universal dynamic scaling. It is further demonstrated both in a two-body system analytically and in a many-body system numerically. For the latter one, we calculate the dynamics of quantum gases quenched from the zero interaction to a finite interaction via the non-equilibrium high-temperature virial expansion. A dynamic scaling of the momentum distribution appears in certain momentum-time windows at unitarity as well as in the weak interacting limit. Remarkably, this universal scaling dynamics persists approximately with smaller scaling exponents even if the scaling symmetry is fairly broken. Our findings may offer a new perspective to interpret the related experiments. We also study the Contact dynamics in the BEC–BCS crossover. Surprisingly, the half-way time displays a maximum near unitarity while some damping oscillations occur on the BEC side due to the dimer state, which can be used to detect possible two-body bound states in experiments.

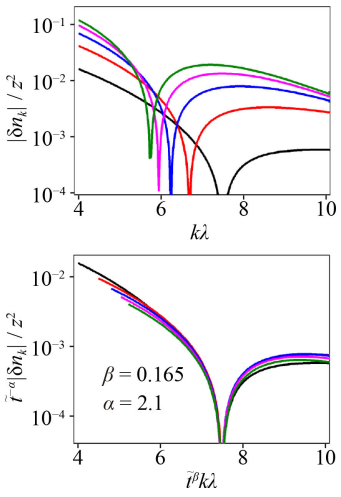

Keywords dynamic scaling, Contact dynamics, quantum gases, cold atom, quench dynamics, virial expansion, continuous scaling symmetry

1 Introduction

Quench dynamics refers to the evolution of a closed system after a sudden change of either the initial state or the Hamiltonian. Given its simple operation in experiments, it becomes one of the most studied non-equilibrium dynamics, especially in ultracold atomic gases [1–9]. The advance in experiments further prompts extensive theoretical studies [10–33]. For instance, the Cambridge group observed several universal phenomena in a three-dimensional (3D) Bose gas quenched from noninteracting to unitarity, such as the exponential form of the momentum distribution at the final steady state [3]. Later, the low temperature condensed part and the thermal gas part of the data are respectively explained by using the time-dependent Bogoliubov theory [23, 24] and the non-equi-

Higher Education Press

arXiv: 2203.14245
https://doi.org/10.1007/s11467-023-1341-z

librium high-temperature virial expansion [27]. On the other hand, some characteristics of the quenched Hamiltonian can lead to novel dynamical phenomena [34–38]. For instance, the Chern number of a topological insulator can be revealed by the linking number in quench dynamics [35–37]. The discrete scaling symmetry of the quenched Hamiltonian may give rise to a dynamical fractal [38].

Recently, universal scaling dynamics is observed in quenched Bose gases [4–7, 9]. The scaling property of spin correlations is investigated both in a quasi-1D [4] and 2D [9] spinor Bose gas, while other works demonstrate the dynamic scaling behavior of the momentum distribution in 1D [5], 2D [7] and 3D [6] Bose gases respectively. Specifically, the evolution of the momentum distribution exhibits a spatiotemporal self-similar scaling feature in certain momentum-time windows, which is analogous to the spatial scaling around the critical point of phase transition [39, 40]. The latter arises from the continuous scaling invariance of the system emerged at the critical point, where the correlation length is divergent. The scaling dynamics has been studied in various systems by a number of theoretical works [41–53], mainly in the framework of non-thermal fixed points. However, there are some disagreements between the theory and the experiment, for example, the scaling exponent [5, 6]. On the other hand, the possible relation between the scaling symmetry and the dynamic scaling has not been discussed yet. If the Hamiltonian $\hat{H}(\mathcal{P})$ has a continuous scaling symmetry, i.e., $\hat{H}(\zeta\mathcal{P}) = \zeta^{\beta}\hat{H}(\mathcal{P})$ with a scaling exponent β (ζ is a positive constant), it can play an important role in quench dynamics through the time-evolution operator $\mathrm{e}^{-\mathrm{i}t\hat{H}}$.

In this letter we investigate this problem by deriving a theorem that connects the continuous scaling symmetry of the quenched Hamiltonian and the initial density matrix to the dynamic scaling of the momentum distribution. We further demonstrate its validity both in a two-body system and in a many-body system. Surprisingly, even if the scaling symmetry required by the theorem is fairly broken, an approximate scaling dynamics can still occur with modified scaling exponents in certain momentum-time windows, which offers a new perspective to interpret the experimental observations. At last, we calculate the Contact dynamics to investigate how the short-range correlations are built up in quenched quantum gases [11, 14, 18, 25], since the Contact is a universal quantity to characterize the property of short-range interactions [54, 55]. Recently, the Contact dynamics also receives the experimental interest [1, 56–58].

2 Universal dynamic scaling

2.1 Theorem

If the initial density matrix $\rho_0 = \int \mathrm{d}\kappa w_\kappa |\psi_\kappa\rangle\langle\psi_\kappa|$ and the quenched Hamiltonian $\hat{H}(\boldsymbol{p}_1, \boldsymbol{p}_2, ...)$ both have a continuous scaling symmetry, i.e.,

$$\begin{cases} w_{\zeta\kappa} = \zeta^{\delta} w_\kappa, \\ \hat{H}(\zeta\boldsymbol{p}_1, \zeta\boldsymbol{p}_2, ...) = \zeta^{\gamma}\hat{H}(\boldsymbol{p}_1, \boldsymbol{p}_2, ...), \end{cases}$$

where, δ and γ denote the scaling exponents. The momentum distribution $n(\boldsymbol{k}, t)$ will exhibit a dynamic scaling behavior in the momentum-time domain, which can be expressed as

$$n(\boldsymbol{k}, t) = \tilde{t}^{\alpha} n(\tilde{t}^{\beta}\boldsymbol{k}, t_0) \tag{1}$$

with $\beta = 1/\gamma$ and $\alpha = 2d/\gamma$. Here, $\boldsymbol{\kappa}$ represents the set of the quantum numbers for the eigenstate $|\psi_\kappa\rangle$. For example, for non-interacting quantum gases, $\kappa = \{\boldsymbol{p}_1, \boldsymbol{p}_2, ...\}$, and for an interacting two-body system with no bound states, $\kappa = \{\boldsymbol{P}, \boldsymbol{q}\}$ with $\boldsymbol{P}$ and $\boldsymbol{q}$ being the total and relative momentum respectively. ζ is a positive number (i.e., the scaling factor). $\tilde{t} = t/t_0$ and d denotes the dimensionality of the system. The proof is displayed in the following.

For a given initial density matrix $\rho_0 = \int \mathrm{d}\kappa w_\kappa |\psi_\kappa\rangle\langle\psi_\kappa|$ at time $t = 0$, the dynamics of the momentum distribution $n(\boldsymbol{k}, t)$ governed by the quenched Hamiltonian $\hat{H}$ at time $t > 0$ can be expressed as

$$n(\boldsymbol{k}, t) = \int \mathrm{d}\kappa w_\kappa \langle\psi_\kappa|\mathrm{e}^{\mathrm{i}t\hat{H}}\hat{n}_{\boldsymbol{k}}\mathrm{e}^{-\mathrm{i}t\hat{H}}|\psi_\kappa\rangle. \tag{2}$$

For simplicity, we define a scaling operator $\hat{S}_\zeta$ as $\langle\boldsymbol{p}_1, \boldsymbol{p}_2, ...|\hat{S}_\zeta|\phi_\kappa\rangle = \langle\boldsymbol{p}_1/\zeta, \boldsymbol{p}_2/\zeta, ...|\phi_\kappa\rangle \equiv \zeta^{Nd}\langle\boldsymbol{p}_1, \boldsymbol{p}_2, ...|\phi_{\zeta\kappa}\rangle$, with N being the total particle number (see the Appendix). By inserting the basis of the eigenstates of the quenched Hamiltonian $\hat{H}$, one can connect the momentum distribution $n(\boldsymbol{k}, t)$ with $n(\zeta\boldsymbol{k}, t\zeta^{-\gamma})$, which is displayed as follows (see the Appendix):

$$n(\boldsymbol{k}, t) = \zeta^{2d} n(\zeta\boldsymbol{k}, t\zeta^{-\gamma}) \equiv \tilde{t}^{\alpha} n(\tilde{t}^{\beta}\boldsymbol{k}, t_0). \tag{3}$$

Note that $\delta = -Nd$ from the constraint $\int \mathrm{d}\kappa w_\kappa = 1$. Here, we have used the property that $|\phi_{\zeta\kappa}\rangle$ is also the eigenfunc tion of the Hamiltonian with the eigenvalue $\zeta^{\gamma}E_\kappa$ [59]. Afterwords, we demonstrate this theorem by directly calculating the quench dynamics of the momentum distribution in a two-body system as well as in a many-body system via the framework of the high-temperature virial expansion.

2.2 Two-body system

We first consider a two-body system with equal mass (m) and an s-wave interaction between them. Essentially, it can be transformed into a one-body problem and the Hamiltonian can be written as $\hat{H} = -\nabla^2/m + \hat{V}(\boldsymbol{r})$ in the relative coordinate. We take the reduced Planck constant and the Boltzmann constant equal to unity for convenience in this paper. If the system is quenched to a finite scattering length a_s at $t = 0$ with an initial state $|\boldsymbol{k} = 0\rangle$, the momentum distribution $n(\boldsymbol{k}, t)$ for finite

momenta ($\boldsymbol{k}>0$) after the quench can be expressed as

$$n(\boldsymbol{k},t)=\left|\frac{1}{2\pi\mathrm{i}}\int_{-\infty}^{+\infty}\mathrm{d}\omega\frac{t_2(s)\mathrm{e}^{-\mathrm{i}\omega t}}{s(s-\varepsilon_{\mathbf{k}})}\right|^2 \tag{4}$$

with the two-body scattering matrix

$$t_2(s)=\frac{4\pi}{m}\frac{1}{a_s^{-1}-\sqrt{-ms}}. \tag{5}$$

Here, $s=\omega+\mathrm{i}0^+$ and $\varepsilon_{\boldsymbol{k}}=\boldsymbol{k}^2/m$. For any finite scattering length, the dynamics of the momentum distribution does not follow Eq. (1), due to the breakdown of the scale invariance. However, in the unitary limit ($a_s\to\infty$), the scale invariance recovers and Eq. (4) can be simplified to

$$n(\boldsymbol{k},t)=\frac{64\pi t}{mk^4}\left|F\left(\frac{1-\mathrm{i}}{\sqrt{2m}}k\sqrt{t}\right)\right|^2, \tag{6}$$

where, the function $F(z)=1-\frac{\sqrt{\pi}}{2}\frac{\mathrm{erf}(z)}{z}\mathrm{e}^{z^2}$ with $\mathrm{erf}(z)$ being the error function. One can see that it indeed satisfies Eq. (1) and exhibits the dynamic scaling with the scaling exponents $\beta=1/2$ and $\alpha=3$ as the theorem says.

If one considers the weak interacting limit, $a_s\to 0$, to the lowest order, the momentum distribution can be written as

$$n(\boldsymbol{k},t)=\frac{32\pi^2a_s^2}{k^4}\left[1-\cos\left(\frac{k^2t}{m}\right)\right]. \tag{7}$$

Remarkably, it also displays the dynamic scaling behavior but with the scaling exponents $\beta=1/2$ and $\alpha=2$. Because the scattering length is much smaller than other relevant length scales, the system remains scale-invariant approximately and our theorem is still valid in such cases. But the scaling exponents can depend on the specific approximation, which is also indicated in Eq. (3).

2.3 Many-body system

For a many-body system, the particle density (or the distance between nearest particles) introduces a new length scale, which generally prevents the system from owning the continuous scaling symmetry, such as the non-interacting or unitary Fermi gas. However, in the low-density limit or the high-energy regime, the influence of this length scale can be negligible and the many-body system may also exhibit scale invariance, similar to the two-body system. In the following, we employ the high-temperature virial expansion to demonstrate the dynamic scaling, where our theorem is applicable.

If one considers that a quantum gas is quenched from a non-interacting Hamiltonian $\hat{H}_0$ with an equilibrium state to an interacting Hamiltonian $\hat{H}$ at time $t=0$, the evolution of the momentum distribution $n(\boldsymbol{k},t)$ for $t>0$ can be expressed as

$$n(\boldsymbol{k},t)=\frac{\mathrm{Tr}[\mathrm{e}^{-\beta(\hat{H}_0-\mu\hat{N})}\mathrm{e}^{\mathrm{i}t\hat{H}}\hat{n}_{\boldsymbol{k}}\mathrm{e}^{-\mathrm{i}t\hat{H}}]}{\mathrm{Tr}[\mathrm{e}^{-\beta(\hat{H}_0-\mu\hat{N})}]}. \tag{8}$$

Here $\beta=1/(k_BT)$ with T being the temperature. μ and N are the chemical potential and the total number of particles, respectively. At high temperature, it can be expanded in powers of the fugacity $z=\mathrm{e}^{\beta\mu}\ll 1$ in the framework of virial expansion [27]. Next, we will consider the change of the momentum distribution $\delta n(\boldsymbol{k},t)=n(\boldsymbol{k},t)-n(\boldsymbol{k},0)$ for simplicity, since it represents the property of the quenched Hamiltonian $\hat{H}$. To the second order of z, it can be expressed as

$$\begin{aligned}\delta n(\boldsymbol{k},t)=&2z^2\sum_{\boldsymbol{k}_1,\boldsymbol{k}_2}f(\boldsymbol{k}_1)f(\boldsymbol{k}_2)\\&\cdot\{2\mathrm{Re}[g(\boldsymbol{k}_1,\boldsymbol{k}_2,t)]\delta_{\boldsymbol{k}_1,\boldsymbol{k}}+|g(\boldsymbol{k}_1,\boldsymbol{k}_2,t)|^2\}\end{aligned} \tag{9}$$

with

$$g(\boldsymbol{k}_1,\boldsymbol{k}_2,t)=\frac{1}{2\pi\mathrm{i}}\int_{-\infty}^{+\infty}\mathrm{d}\omega\frac{t_2(s)\mathrm{e}^{-\mathrm{i}t(\omega-\varepsilon_{\boldsymbol{q}_1})}}{(s-\varepsilon_{\boldsymbol{q}_1})(s-\varepsilon_{\boldsymbol{q}_2})}. \tag{10}$$

Here, $s=\omega+\mathrm{i}0^+$, $\boldsymbol{q}_1=(\boldsymbol{k}_1-\boldsymbol{k}_2)/2$, $\boldsymbol{q}_2=\boldsymbol{k}-(\boldsymbol{k}_1+\boldsymbol{k}_2)/2$, $\varepsilon_{\boldsymbol{q}}=\boldsymbol{q}^2/m$ and $f(\boldsymbol{k}_1)=\mathrm{e}^{-2\beta\varepsilon_{\boldsymbol{k}_1}}$. One can calculate Eq. (9) numerically to obtain the dynamics of the momentum distribution.

The initial distribution function $f(\boldsymbol{k}_1)=\mathrm{e}^{-2\beta\varepsilon_{\boldsymbol{k}_1}}$ does not have a scaling symmetry. However, if one considers the large momentum region $k\lambda\gg 1$ and $t/t_\lambda\ll 1(t_\lambda=1/T)$, this Gaussian function can be regarded as a Dirac delta function approximately and the scaling symmetry recovers. Therefore, according to our theorem, a scaling dynamics can occur at unitarity [60] and indeed this is ture as shown in Fig. 1. Moreover, we calculate the results in the whole BEC–BCS crossover. The finite scattering length breaks the scaling symmetry of the Hamiltonian and the dynamic scaling disappears. Nevertheless, in the weak interacting limit, i.e., $a_s\to 0$, the scattering length is much smaller than all other relevant length scales in the system and the scaling symmetry recovers approximately, which further leads to the recurring scaling dynamics. Note that to the lowest order (i.e., the order of a_s^2), $\beta=1/2$ and $\alpha=2$ due to the prefactor a_s^2 in this approximation, which does not follow the theorem quantitatively. All the numerical results agree well with the above analysis based on the theorem. Our results imply that the scaling dynamics can occur in a specific momentum-time window, as long as the initial state and the Hamiltonian are scale-invariant approximately in this domain.

Actually, if one takes the initial distribution function as $f(\boldsymbol{k}_1)=\delta(\boldsymbol{k}_1)$ mathematically, Eq. (9) can be simplified to

$$\delta n(\boldsymbol{k},t)=2z^2|g(0,0,t)|^2, \tag{11}$$

which is the same with the result of the two-body

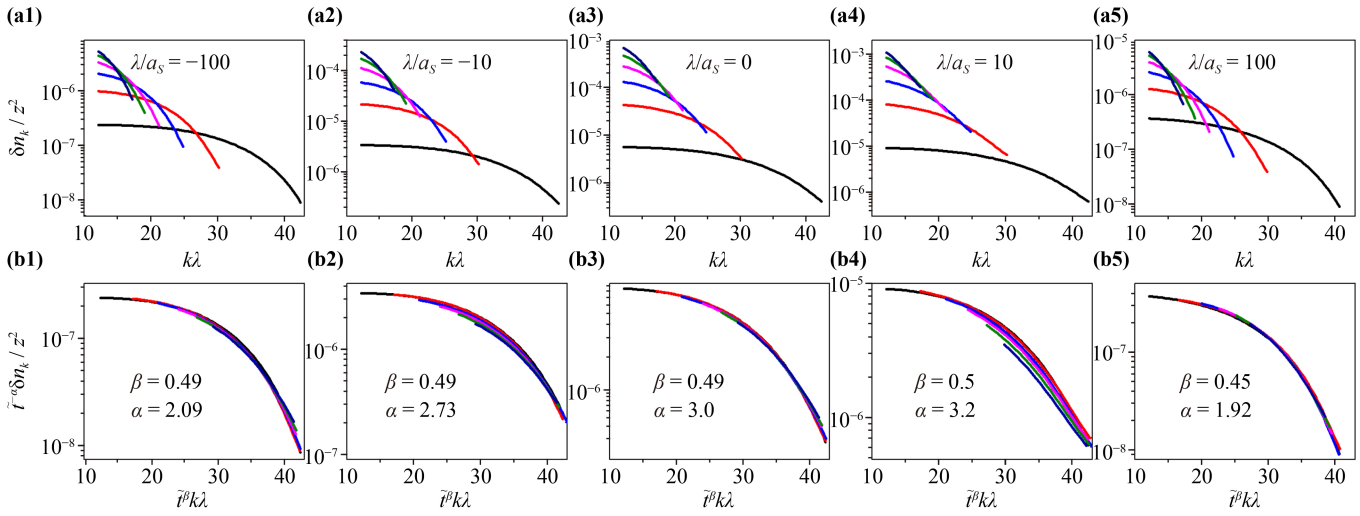

Fig. 1 The momentum distribution δn_k at the large momentum region for various times $t/t_\lambda = 0.02$ (black), 0.04 (red), 0.06 (blue), 0.08 (pink), 0.10 (green), 0.12 (navy) in the quench dynamics of quantum gases. Here, $\lambda = \sqrt{2\pi/(mT)}$ is the thermal wavelength, while $t_\lambda = 1/T$. $\tilde{t} = t/t_0$ with $t_0/t_\lambda = 0.02$. The results in the BEC-BCS crossover are displayed with the scattering length labelled in the first row. In the second row, the corresponding scalings of both the horizontal and vertical axes are taken via Eq. (1), to demonstrate whether there exists a dynamic scaling behavior. The scaling exponents α and β are shown in the corresponding graphs.

system [see Eq. (4)], except the prefactor $2z^2$. Thus, it is straightforward to show that $\delta n(\boldsymbol{k}, t) = \tilde{t}^3 \delta n(\tilde{t}^{1/2}\boldsymbol{k}, t_0)$ for all finite momenta at unitarity and $\delta n(\boldsymbol{k}, t) = \tilde{t}^2 \delta n(\tilde{t}^{1/2}\boldsymbol{k}, t_0)$ as $a_s \to 0$ (to the order of a_s^2), which are in excellent agreement with our numerical results (see Fig. 1).

2.4 Approximate dynamic scaling

Surprisingly, even if the scale-invariant condition is not strictly satisfied, an approximate scaling dynamics can still occur in certain momentum-time windows as shown in Fig. 2. If one considers the momentum region $k\lambda \in [4, 10]$, the strict dynamic scaling is not expected given the missing scaling invariance of the initial density matrix. However, there exists an approximate dynamic scaling with modified scaling exponents, which may arise from the approximate scaling behaviors of the initial density matrix (or the main contributing part) with different scaling exponents in certain momentum regions.

On the one hand, it demonstrates that the dynamic scaling can be robust against the proper breakdown of the continuous scaling symmetry for either the initial density matrix or the Hamiltonian. On the other hand, it could be closely related to the recent experimental observations [5, 6], since the experimental condition does not strictly satisfy the scaling symmetry either and the scaling exponents vary significantly in different systems. Here, we would like to emphasize that there are two key features, on which both the experiment and our theory agree well with each other qualitatively. One is that both the scaling exponents β and α are smaller than that

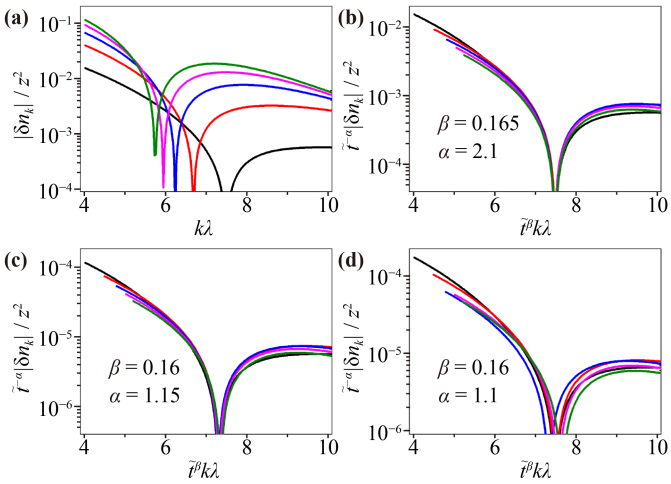

Fig. 2 The quench dynamics of the momentum distribution $|\delta n_k|$ at finite momentum region for various times $t/t_\lambda = 0.1$ (black), 0.2 (red), 0.3 (blue), 0.4 (pink), 0.5 (green). The results for the unitarity are plotted with unscaled axes **(a)** and scaled axes **(b)**, while they are only demonstrated in scaled axes for $\lambda/a_s = -100$ **(c)** and $\lambda/a_s = 100$ **(d)**. According to the theorem, they are not expected to display any strict dynamic scaling behavior, due to the breakdown of the scale invariance of the initial density matrix. However, an approximate scaling dynamics can still be seen in all three cases with smaller scaling exponents α and β displayed in the corresponding graphs.

of the strict dynamic scaling in the theorem. The other is the scaling exponents depend on the chosen momentum-time windows. Therefore, our results provide a new perspective to interpret the experimental observations.

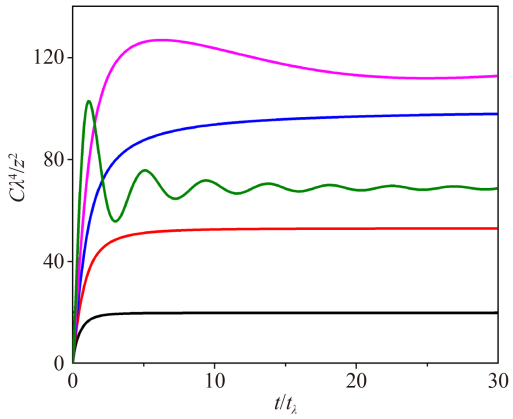

Fig. 3 The Contact dynamics after the quench for $\lambda/a_s =$ –3 (black), –1 (red), 0 (blue), 1 (pink), 3 (green). They all start from zero and approach to a steady value at long times. On the BEC side, they exhibit damping oscillations.

3 Contact dynamics

In this section, we further study universal features of the Contact dynamics in quenched quantum gases, which correspond to the large-momentum limit. In the framework of high-temperature virial expansion, it can be directly obtained from the momentum distribution, through the relation $C(t) = \lim_{k\to\infty} k^4 \delta n(\boldsymbol{k}, t)$. To the second order of z, the Contact dynamics in the BEC–BCS crossover is displayed in Fig. 3. Owing to the initial non-interacting equilibrium state, they all start from zero and gradually approach to a steady state at long evolution times. At unitarity, one can derive an analytic form, expressed as

$$C(a_s \to \infty) = \frac{64z^2}{\lambda^4} \arctan\left(\frac{t}{t_\lambda}\right). \tag{12}$$

In the whole BEC–BCS crossover, as $t \to 0$, the Contact can be expanded in powers of t. To the lowest order, it can be written as

$$C(t \to 0) = \frac{64z^2}{\lambda^4 t_\lambda} t, \tag{13}$$

which is independent of the scattering length and consistent with Ref. [61]'s result. Actually in this limit, the momentum distribution $\delta n(\boldsymbol{k}, t) \approx [64z^2/(\lambda^4 t_\lambda)]t/k^4$ for large momenta can be obtained. As expected, it satisfies the dynamic scaling relation [see Eq. (1)], because the scattering length is much larger than other relevant length scales in this regime and the system can be regarded as being scale-invariant. On the BEC side, there exist some damping oscillations, which are associated with the dimer state. Roughly speaking, they result from the coupling between the dimer state and the scattering states after the quench. The decoherence of the scattering states further leads to the damping, due to different scattering energies.

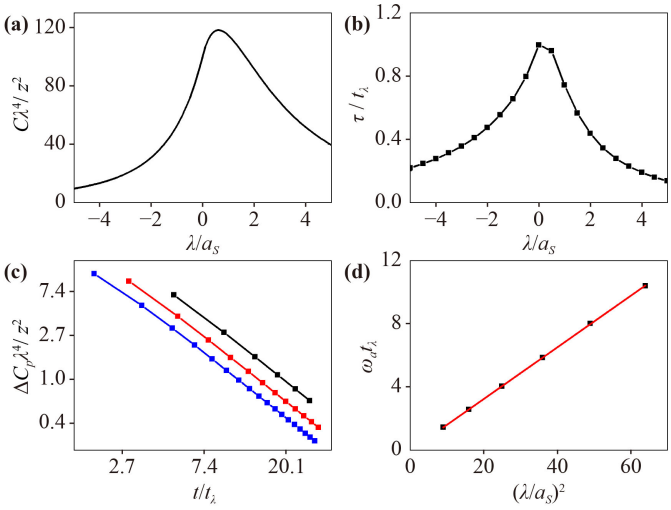

Fig. 4 The Contact dynamics in the BEC-BCS crossover. **(a)** The Contact at infinite time ($t \to \infty$) in the whole BEC-BCS crossover, obtained from Eq. (14). **(b)** The half-way time τ as a function of the interaction. **(c)** The relative value at the peak $\Delta C_p = C_p - C(t \to \infty)$ for $\lambda/a_s = 3$ (black), 4 (red), 5 (blue), which obeys a power-law decay with the same power approximately. **(d)** The frequencies of oscillations at various interactions on the BEC side, with a linear fitting (red line).

For $t \to \infty$, one can obtain the Contact of the final steady state, which can be written analytically as

$$C(\infty) = \frac{z^2}{\lambda^4}\left\{\left[32\pi - \frac{64\lambda^2}{a_s^2}\Theta(a_s)\right] + \frac{16\sqrt{2}\lambda}{a_s}\left[\pi + \frac{2\lambda^2}{a_s^2}\Theta(a_s)\right] \mathrm{e}^{\frac{\lambda^2}{2\pi a_s^2}} \mathrm{erfc}\left(\frac{\lambda}{\sqrt{2\pi}|a_s|}\right)\right\}. \tag{14}$$

Here, $\Theta(x)$ and $\mathrm{erfc}(x)$ are respectively the unit step function and the complementary error function. It exhibits a maximum around the unitarity, as displayed in Fig. 4(a). We further define a half-way time τ as $C(t = \tau) = C(\infty)/2$ to quantify how fast the Contact evolves [3, 27]. The results for the BEC–BCS crossover are displayed in Fig. 4(b). Surprisingly, a maximum occurs around the unitarity, indicating the evolving time is determined mainly by the difference between the final state and the initial state [see Fig. 4(a)], instead of the interaction strength.

We quantitatively investigate the damping oscillations on the BEC side to reveal the relation between oscillations and the dimer state. The relative values at the peak $\Delta C_p = C_p - C(\infty)$ obey a universal power-law decay with the same power approximately for various interactions [see Fig. 4(c)], implying the intial state plays an important role on the damping rate instead of the interaction. However, the frequencies are proportional to a_s^{-2} approxi-

mately [see Fig. 4(d)], which is associated to the energy difference between the dimer state and the scattering state. It will be determined by the dimer's binding energy when the energy of the scattering state can be negligible. Therefore, these oscillations of the Contact dynamics can be used as a tool to detect possible dimer states in experiments.

4 Conclusion

In summary, we find a theorem showing that the continuous scale invariance of the Hamiltonian and the initial density matrix can give rise to the universal scaling dynamics. We first demonstrate it in the two-body system analytically. Then, for quantum gases quenched from the non-interacting equilibrium state, the dynamic scaling appears at large momentum region for both the unitary limit and the weak interacting limit. Remarkably, an approximate dynamic scaling with smaller scaling exponents is also found at finite momentum region, which may offer a new interpretation to the experimental observations. Our results can also guide the future exploration of the scaling dynamics in various systems. The calculated Contact dynamics exhibits several novel features such as a maximum of the half-way time around the unitary limit and the damping oscillations on the BEC side, which can be explored by the experiment in near future [3, 6, 56, 57].

Declarations The authors declare that they have no competing interests and there are no conflicts.

Acknowledgements We thank Zheyu Shi, Pengfei Zhang, Ran Qi, Zhiyuan Yao, Lei Pan, Ren Zhang, and Hui Zhai for inspiring discussion. The project was supported by the National Natural Science Foundation of China (NSFC) (Grant No. 12004049) and the Fund of State Key Laboratory of IPOC (BUPT) (Nos. 600119525 and 505019124).

Appendix: Proof of the theorem

In this appendix, we perform the derivation of the theorem (i.e., Eq. (3) in the main text) step by step. We first display the scaling behavior of each term separately and then put them together to give the final result. Given the quenched Hamiltonian is scale-invariant, if the wavefunction $|\phi_\eta\rangle$ is an eigenfunction of the Hamiltonian with the eigenvalue E_η(η denotes Nd quantum numbers with N and d being the total particle number and the dimensionality respectively), a scaled wavefunction $|\phi_{\zeta\eta}\rangle$ (ζ is a positive number) will also be an eigenfunction with the eigenvalue $E_{\zeta\eta}=\zeta^\gamma E_\eta$ [59]. Therefore, if assuming $\phi_{\zeta\eta}(\zeta\boldsymbol{k}_1,\cdots,\zeta\boldsymbol{k_N})=A\phi_\eta(\boldsymbol{k}_1,\cdots,\boldsymbol{k_N})$ (A is a real number), one can have

$$\begin{aligned}\langle\phi_{\zeta\eta_1}|\phi_{\zeta\eta_2}\rangle=&\int \mathrm{d}\boldsymbol{k}_1\cdots\mathrm{d}\boldsymbol{k_N}\phi^*_{\zeta\eta_1}(\boldsymbol{k}_1,\cdots,\boldsymbol{k_N})\\&\cdot\phi_{\zeta\eta_2}(\boldsymbol{k}_1,\cdots,\boldsymbol{k_N})\\=&\zeta^{Nd}\int \mathrm{d}\boldsymbol{k}_1\cdots\mathrm{d}\boldsymbol{k_N}\phi^*_{\zeta\eta_1}(\zeta\boldsymbol{k}_1,\cdots,\zeta\boldsymbol{k_N})\\&\cdot\phi_{\zeta\eta_2}(\zeta\boldsymbol{k}_1,\cdots,\zeta\boldsymbol{k_N})\\=&\zeta^{Nd}\int \mathrm{d}\boldsymbol{k}_1\cdots\mathrm{d}\boldsymbol{k_N}A\phi^*_{\eta_1}(\boldsymbol{k}_1,\cdots,\boldsymbol{k_N})\\&\cdot A\phi_{\eta_2}(\boldsymbol{k}_1,\cdots,\boldsymbol{k_N})\\=&A^2\zeta^{Nd}\langle\phi_{\eta_1}|\phi_{\eta_2}\rangle.\end{aligned}\tag{15}$$

According to the condition $\langle\phi_{\zeta\eta_1}|\phi_{\zeta\eta_2}\rangle=\delta(\zeta\eta_1-\zeta\eta_2)=\zeta^{-Nd}\delta(\eta_1-\eta_2)$, one can obtain $A=\zeta^{-Nd}$ and $\langle\phi_{\zeta\eta_1}|\phi_{\zeta\eta_2}\rangle=\zeta^{-Nd}\langle\phi_{\eta_1}|\phi_{\eta_2}\rangle$. Based on this, it is straightforward to derive that

$$\langle\psi_\kappa|\mathrm{e}^{\mathrm{i}t\hat{H}}|\phi_\eta\rangle=\zeta^{Nd}\langle\psi_{\zeta\kappa}|\mathrm{e}^{\mathrm{i}t\zeta^{-\gamma}\hat{H}}|\phi_{\zeta\eta}\rangle.\tag{16}$$

For the term involved with the momentum distribution, it can be transformed as follows:

$$\begin{aligned}\langle\phi_{\eta_1}|\hat{n}_{\boldsymbol{k}}|\phi_{\eta_2}\rangle=&\int \mathrm{d}\boldsymbol{k}_1\cdots\mathrm{d}\boldsymbol{k_N}\phi^*_{\eta_1}(\boldsymbol{k}_1,\cdots,\boldsymbol{k_N})\\&\cdot\sum_m\delta(\boldsymbol{k_m}-\boldsymbol{k})\phi_{\eta_2}(\boldsymbol{k}_1,\cdots,\boldsymbol{k_N})\\=&\sum_m\int \mathrm{d}\boldsymbol{k_m}f_{\eta_1,\eta_2}(\boldsymbol{k_m})\delta(\boldsymbol{k_m}-\boldsymbol{k})\\=&\sum_m\int \mathrm{d}\boldsymbol{k_m}\zeta^{3d}f_{\zeta\eta_1,\zeta\eta_2}(\zeta\boldsymbol{k_m})\delta(\zeta\boldsymbol{k_m}-\zeta\boldsymbol{k})\\=&\zeta^{2d}\sum_m\int \mathrm{d}\boldsymbol{k_m}f_{\zeta\eta_1,\zeta\eta_2}(\boldsymbol{k_m})\delta(\boldsymbol{k_m}-\zeta\boldsymbol{k})\\=&\zeta^{2d}\langle\phi_{\zeta\eta_1}|\hat{n}_{\zeta\boldsymbol{k}}|\phi_{\zeta\eta_2}\rangle.\end{aligned}\tag{17}$$

Here, we have first integrated over all other momenta (except $\boldsymbol{k_m}$) and then regularized the scaling divergent term [see Eq. (15)], to obtain $f_{\eta_1,\eta_2}(\boldsymbol{k_m})=\int \mathrm{d}\boldsymbol{k}_1\cdots\mathrm{d}\boldsymbol{k}_{m-1}\,\mathrm{d}\boldsymbol{k}_{m+1}\cdots\mathrm{d}\boldsymbol{k_N}\phi^*_{\eta_1}(\boldsymbol{k}_1,\cdots,\boldsymbol{k_N})\phi_{\eta_2}(\boldsymbol{k}_1,\cdots,\boldsymbol{k_N})$ in one-particle space, which satisfies $f_{\eta_1,\eta_2}(\boldsymbol{k_m})=\zeta^{2d}f_{\zeta\eta_1,\zeta\eta_2}(\zeta\boldsymbol{k_m})$.

With Eqs. (16) and (17), one can derive the dynamic scaling of the momentum distribution as follows:

$$\begin{aligned}n(\boldsymbol{k},t)=&\int \mathrm{d}\kappa w_\kappa\langle\psi_\kappa|\mathrm{e}^{\mathrm{i}t\hat{H}}\hat{n}_{\boldsymbol{k}}\mathrm{e}^{-\mathrm{i}t\hat{H}}|\psi_\kappa\rangle\\=&\int \mathrm{d}\kappa\int \mathrm{d}\eta_1\int \mathrm{d}\eta_2 w_\kappa\langle\psi_\kappa|\mathrm{e}^{\mathrm{i}t\hat{H}}|\phi_{\eta_1}\rangle\langle\phi_{\eta_1}|\hat{n}_{\boldsymbol{k}}|\phi_{\eta_2}\rangle\\&\cdot\langle\phi_{\eta_2}|\mathrm{e}^{-\mathrm{i}t\hat{H}}|\psi_\kappa\rangle\\=&\zeta^{2d}\int \mathrm{d}\kappa w_\kappa\langle\psi_\kappa|\mathrm{e}^{\mathrm{i}t\zeta^{-\gamma}\hat{H}}\hat{n}_{\zeta\boldsymbol{k}}\mathrm{e}^{-\mathrm{i}t\zeta^{-\gamma}\hat{H}}|\psi_\kappa\rangle\\=&\zeta^{2d}n(\zeta\boldsymbol{k},t\zeta^{-\gamma})\\\equiv&\tilde{t}^\alpha n(\tilde{t}^\beta\boldsymbol{k},t_0).\end{aligned}\tag{18}$$

Here, $w_\kappa = \zeta^{-\delta} w_{\zeta\kappa}$ with $\delta = -Nd$, which can be obtained from the relation $\int \mathrm{d}\kappa w_\kappa = \zeta^{Nd} \int \mathrm{d}\kappa w_{\zeta\kappa} = \zeta^{Nd+\delta} \int \mathrm{d}\kappa w_\kappa$. We set $\tilde{t} = t/t_0$, the scaling exponent $\beta = 1/\gamma$ and $\alpha = 2d/\gamma = 2d\beta$. Thus, the theorem is proved.

References

1. P. Makotyn, C. E. Klauss, D. L. Goldberger, E. A. Cornell, and D. S. Jin, Universal dynamics of a degenerate unitary Bose gas, *Nat. Phys.* 10(2), 116 (2014)
2. C. Eigen, J. A. P. Glidden, R. Lopes, N. Navon, Z. Hadzibabic, and R. P. Smith, Universal scaling laws in the dynamics of a homogeneous unitary Bose gas, *Phys. Rev. Lett.* 119(25), 250404 (2017)
3. C. Eigen, J. A. Glidden, R. Lopes, E. A. Cornell, R. P. Smith, and Z. Hadzibabic, Universal prethermal dynamics of Bose gases quenched to unitarity, *Nature* 563(7730), 221 (2018)
4. M. Prüfer, P. Kunkel, H. Strobel, S. Lannig, D. Linnemann, C. M. Schmied, J. Berges, T. Gasenzer, and M. K. Oberthaler, Observation of universal dynamics in a spinor Bose gas far from equilibrium, *Nature* 563(7730), 217 (2018)
5. S. Erne, R. Bucker, T. Gasenzer, J. Berges, and J. Schmiedmayer, Universal dynamics in an isolated one-dimensional Bose gas far from equilibrium, *Nature* 563(7730), 225 (2018)
6. J. A. P. Glidden, C. Eigen, L. H. Dogra, T. A. Hilker, R. P. Smith, and Z. Hadzibabic, Bidirectional dynamic scaling in an isolated Bose gas far from equilibrium, *Nat. Phys.* 17(4), 457 (2021)
7. M. Gałka, P. Christodoulou, M. Gazo, A. Karailiev, N. Dogra, J. Schmitt, and Z. Hadzibabic, Emergence of isotropy and dynamic scaling in 2D wave turbulence in a homogeneous Bose gas, *Phys. Rev. Lett.* 129(19), 190402 (2022)
8. D. Wei, A. Rubio-Abadal, B. Ye, F. Machado, J. Kemp, K. Srakaew, S. Hollerith, J. Rui, S. Gopalakrishnan, N. Y. Yao, I. Bloch, and J. Zeiher, Quantum gas microscopy of Kardar–Parisi–Zhang superdiffusion, *Science* 376(6594), 716 (2022)
9. S. Huh, K. Mukherjee, K. Kwon, J. Seo, S. I. Mistakidis, H. R. Sadeghpour, and J. Y. Choi, Classifying the universal coarsening dynamics of a quenched ferromagnetic condensate, arXiv: 2303.05230 (2023)
10. X. Yin and L. Radzihovsky, Quench dynamics of a strongly interacting resonant Bose gas, *Phys. Rev. A* 88(6), 063611 (2013)
11. A. G. Sykes, J. P. Corson, J. P. D'Incao, A. P. Koller, C. H. Greene, A. M. Rey, K. R. Hazzard, and J. L. Bohn, Quenching to unitarity: Quantum dynamics in a three-dimensional Bose gas, *Phys. Rev. A* 89(2), 021601 (2014)
12. A. Rançon and K. Levin, Equilibrating dynamics in quenched Bose gases: Characterizing multiple time regimes, *Phys. Rev. A* 90(2), 021602 (2014)
13. B. Kain and H. Y. Ling, Nonequilibrium states of a quenched Bose gas, *Phys. Rev. A* 90(6), 063626 (2014)
14. J. P. Corson, and J. L. Bohn, Bound-state signatures in quenched Bose–Einstein condensates, *Phys. Rev. A* 91(1), 013616 (2015)
15. F. Ancilotto, M. Rossi, L. Salasnich, and F. Toigo, Quenched dynamics of the momentum distribution of the unitary Bose gas, *Few-Body Syst.* 56(11-12), 801 (2015)
16. X. Yin and L. Radzihovsky, Postquench dynamics and prethermalization in a resonant Bose gas, *Phys. Rev. A* 93(3), 033653 (2016)
17. S. Y. Wu, H. H. Zhong, J. H. Huang, X. Z. Qin, and C. H. Lee, Dynamic fragmentation in a quenched two-mode Bose–Einstein condensate, *Front. Phys.* 11(3), 110301 (2016)
18. V. E. Colussi, J. P. Corson, and J. P. D'Incao, Dynamics of three-body correlations in quenched unitary Bose gases, *Phys. Rev. Lett.* 120(10), 100401 (2018)
19. V. E. Colussi, S. Musolino, and S. J. J. M. F. Kokkelmans, Dynamical formation of the unitary Bose gas, *Phys. Rev. A* 98(5), 051601 (2018)
20. M. Van Regemortel, H. Kurkjian, M. Wouters, and I. Carusotto, Prethermalization to thermalization crossover in a dilute Bose gas following an interaction ramp, *Phys. Rev. A* 98(5), 053612 (2018)
21. J. P. D'Incao, J. Wang, and V. E. Colussi, Efimov physics in quenched unitary Bose gases, *Phys. Rev. Lett.* 121(2), 023401 (2018)
22. S. Musolino, V. E. Colussi, and S. J. J. M. F. Kokkelmans, Pair formation in quenched unitary Bose gases, *Phys. Rev. A* 100(1), 013612 (2019)
23. C. Gao, M. Y. Sun, P. Zhang, and H. Zhai, Universal dynamics of a degenerate Bose gas quenched to unitarity, *Phys. Rev. Lett.* 124(4), 040403 (2020)
24. A. Muñoz de las Heras, M. M. Parish, and F. M. Marchetti, Early-time dynamics of Bose gases quenched into the strongly interacting regime, *Phys. Rev. A* 99(2), 023623 (2019)
25. V. E. Colussi, B. E. van Zwol, J. P. D'Incao, and S. J. J. M. F. Kokkelmans, Bunching, clustering, and the buildup of few-body correlations in a quenched unitary Bose gas, *Phys. Rev. A* 99(4), 043604 (2019)
26. G. Bougas, S. I. Mistakidis, and P. Schmelcher, Analytical treatment of the interaction quench dynamics of two bosons in a two-dimensional harmonic trap, *Phys. Rev. A* 100(5), 053602 (2019)
27. M. Y. Sun, P. Zhang, and H. Zhai, High temperature virial expansion to universal quench dynamics, *Phys. Rev. Lett.* 125(11), 110404 (2020)
28. V. E. Colussi, H. Kurkjian, M. Van Regemortel, S. Musolino, J. van de Kraats, M. Wouters, and S. J. J. M. F. Kokkelmans, Cumulant theory of the unitary Bose gas: Prethermal and Efimovian dynamics, *Phys. Rev. A* 102(6), 063314 (2020)
29. G. Bougas, S. I. Mistakidis, G. M. Alshalan, and P. Schmelcher, Stationary and dynamical properties of two harmonically trapped bosons in the crossover from two dimensions to one, *Phys. Rev. A* 102(1), 013314 (2020)
30. S. Musolino, H. Kurkjian, M. Van Regemortel, M. Wouters, S. J. J. M. F. Kokkelmans, and V. E. Colussi, Bose–Einstein condensation of Efimovian triples in the unitary Bose gas, *Phys. Rev. Lett.* 128(2), 020401 (2022)

31. T. Enss, N. Cuadra Braatz, and G. Gori, Complex scaling flows in the quench dynamics of interacting particles, *Phys. Rev. A* 106(1), 013308 (2022)
32. G. W. Fan, X. L. Chen, and P. Zou, Probing two Higgs oscillations in a one-dimensional Fermi superfluid with Raman-type spin–orbit coupling, *Front. Phys.* 17(5), 52502 (2022)
33. Y. M. Hu, Y. F. Fei, X. L. Chen, and Y. B. Zhang, Collisional dynamics of symmetric two-dimensional quantum droplets, *Front. Phys.* 17(6), 61505 (2022)
34. D. A. Abanin, E. Altman, I. Bloch, and M. Serbyn, Many-body localization, thermalization, and entanglement, *Rev. Mod. Phys.* 91(2), 021001 (2019)
35. C. Wang, P. F. Zhang, X. Chen, J. L. Yu, and H. Zhai, Scheme to measure the topological number of a Chern insulator from quench dynamics, *Phys. Rev. Lett.* 118(18), 185701 (2017)
36. W. Sun, C. R. Yi, B. Z. Wang, W. W. Zhang, B. C. Sanders, X. T. Xu, Z. Y. Wang, J. Schmiedmayer, Y. Deng, X. J. Liu, S. Chen, and J. W. Pan, Uncover topology by quantum quench dynamics, *Phys. Rev. Lett.* 121(25), 250403 (2018)
37. M. Tarnowski, F. N. Unal, N. Fläschner, B. S. Rem, A. Eckardt, K. Sengstock, and C. Weitenberg, Measuring topology from dynamics by obtaining the Chern number from a linking number, *Nat. Commun.* 10(1), 1728 (2019)
38. C. Gao, H. Zhai, and Z. Y. Shi, Dynamical fractal in quantum gases with discrete scaling symmetry, *Phys. Rev. Lett.* 122(23), 230402 (2019)
39. K. Huang, Statistical Mechanics, John Wiley & Sons, New York, 1987
40. S. Sachdev, Quantum Phase Transitions, Cambridge University Press, Cambridge, 1999
41. R. Micha and I. I. Tkachev, Turbulent thermalization, *Phys. Rev. D* 70(4), 043538 (2004)
42. J. Berges, A. Rothkopf, and J. Schmidt, Nonthermal fixed points: Effective weak coupling for strongly correlated systems far from equilibrium, *Phys. Rev. Lett.* 101(4), 041603 (2008)
43. B. Nowak, J. Schole, D. Sexty, and T. Gasenzer, Nonthermal fixed points, vortex statistics, and superfluid turbulence in an ultracold Bose gas, *Phys. Rev. A* 85(4), 043627 (2012)
44. B. Nowak, J. Schole, and T. Gasenzer, Universal dynamics on the way to thermalization, *New J. Phys.* 16(9), 093052 (2014)
45. J. Berges, K. Boguslavski, S. Schlichting, and R. Venugopalan, Universality far from equilibrium: From superfluid Bose gases to heavy-ion collisions, *Phys. Rev. Lett.* 114(6), 061601 (2015)
46. A. P. Orioli, K. Boguslavski, and J. Berges, Universal self-similar dynamics of relativistic and nonrelativistic field theories near nonthermal fixed points, *Phys. Rev. D* 92(2), 025041 (2015)
47. I. Chantesana, A. P. Orioli, and T. Gasenzer, Kinetic theory of nonthermal fixed points in a Bose gas, *Phys. Rev. A* 99(4), 043620 (2019)
48. A. N. Mikheev, C. M. Schmied, and T. Gasenzer, Low-energy effective theory of nonthermal fixed points in a multicomponent Bose gas, *Phys. Rev. A* 99(6), 063622 (2019)
49. C. M. Schmied, A. N. Mikheev, and T. Gasenzer, Nonthermal fixed points: Universal dynamics far from equilibrium, *Int. J. Mod. Phys. A* 34(29), 1941006 (2019)
50. S. Bhattacharyya, J. F. Rodriguez-Nieva, and E. Demler, Universal prethermal dynamics in Heisenberg ferromagnets, *Phys. Rev. Lett.* 125(23), 230601 (2020)
51. J. Berges, K. Boguslavski, M. Mace, and J. M. Pawlowski, Gauge-invariant condensation in the nonequilibrium quark-gluon plasma, *Phys. Rev. D* 102(3), 034014 (2020)
52. K. Fujimoto, R. Hamazaki, and Y. Kawaguchi, Family–Vicsek scaling of roughness growth in a strongly interacting Bose gas, *Phys. Rev. Lett.* 124(21), 210604 (2020)
53. T. Preis, M. P. Heller, and J. Berges, Stable and unstable perturbations in universal scaling phenomena far from equilibrium, *Phys. Rev. Lett.* 130(3), 031602 (2023)
54. S. Tan, Large momentum part of a strongly correlated Fermi gas, *Ann. Phys.* 323(12), 2971 (2008)
55. S. Zhang and A. J. Leggett, Universal properties of the ultracold Fermi gas, *Phys. Rev. A* 79(2), 023601 (2009)
56. A. B. Bardon, S. Beattie, C. Luciuk, W. Cairncross, D. Fine, N. S. Cheng, G. J. A. Edge, E. Taylor, S. Zhang, S. Trotzky, and J. H. Thywissen, Transverse demagnetization dynamics of a unitary Fermi gas, *Science* 344(6185), 722 (2014)
57. R. J. Fletcher, R. Lopes, J. Man, N. Navon, R. P. Smith, M. W. Zwierlein, and Z. Hadzibabic, Two- and three-body contacts in the unitary Bose gas, *Science* 355(6323), 377 (2017)
58. C. Luciuk, S. Smale, F. Böttcher, H. Sharum, B. A. Olsen, S. Trotzky, T. Enss, and J. H. Thywissen, Observation of quantum-limited spin transport in strongly interacting two-dimensional Fermi gases, *Phys. Rev. Lett.* 118(13), 130405 (2017)
59. F. Werner and Y. Castin, Unitary gas in an isotropic harmonic trap: Symmetry properties and applications, *Phys. Rev. A* 74(5), 053604 (2006)
60. In three-dimensional unitary Bose gas, the scale invariance is only approximate because of the three-body parameter. However, experiments [1–3] show that its contribution can be insignificant in quench dynamics
61. R. Qi, Z. Y. Shi, and H. Zhai, Maximum energy growth rate in dilute quantum gases, *Phys. Rev. Lett.* 126(24), 240401 (2021)